Calculations of effusive-flow patterns. III. Scattering chambers with thin circular apertures

B. P. Mathur,* J. E. Field, and S. O. Colgate
Department of Chemistry, University of Florida, Gainesville, Florida 32611
(Received 26 August 1974)

Values of the gas density profile correction factor α are calculated for a series of cylindrical beam-scattering chambers with identical thin circular apertures.

I. INTRODUCTION

Papers in this series are concerned with the calculation of gas density distributions in steady-state effusive flows. The basic method was given in Paper I[1] and applied to flows in Knudsen cells. Paper II[2] addressed the problem of principal interest to this laboratory, namely, the calculation of scattering-gas density profiles in beam scattering experiments, and presented results for scattering chambers with semi-infinite slits of negligible channel length.

The procedure gives good results subject to the restraints: (a) the chamber walls reflect gas molecules diffusively according to the cosine law; (b) the pressures are sufficiently low that gas phase collisions can be neglected with respect to impacts of gas molecules on the chamber walls; and (c) steady-state conditions prevail. The present report gives results of similar calculations for scattering chambers of a more realistic but still mathematically simple geometry; namely, chambers with identical circular apertures of negligible channel length.

As before, the results are given in terms of the parameter α, which corrects conventional total cross section calculations for nonuniformity in the scattering gas distribution:

$$Q(v_b) = \frac{\ln(I_0/I)R(v_b)}{F_B \alpha n_0 l}, \tag{1}$$

where the notation is the same as that of Paper II.

II. GEOMETRY

The present calculations relate to the geometric arrangement of Fig. 1. All dimensions are reduced in terms of the aperture radius. The source is considered to be uniformly distributed over the cylindrical surface centered around the beam axis and having reduced radius R and reduced length H. This arrangement was chosen because (i) the resultant symmetry simplifies the calculations and (ii) it can be closely simulated in the laboratory by constructing scattering chambers having apertures in the ends of hollow cylindrical plugs which are surrounded by a large annular space to which the scattering gas is delivered.[3] The scattering-gas pressure can conveniently be measured in the annular space by means of a suitable small-volume gauge (thermocouple gauge, Pirani gauge, etc.). The corresponding number density is taken as a measure of n_0 and assumed to be uniform in the above-mentioned annular region.

III. CALCULATIONS

The method of calculation used was the same as that described in Papers I and II. The gradients in the effective gas density over the end walls of the chamber were found by dividing each wall into a number of concentric rings of equal width and following the previously described iterative procedure to find the convergence limit at which each ring receives and reflects gas molecules under steady-state conditions. The resulting densities were taken to be the effective radiative densities at values of r corresponding to the distances from the center of the aperture to the midpoints of the ring cells. In each case the gradient was given analytical form by least-squaring the numerical results to an equation of the form

$$n(H/2, r) = n_0(a_0 + a_1 r + a_2 r^2 + a_3 r^3). \tag{2}$$

In all cases the average deviation of the analytical fit from the numerical values was less than 0.01%. Some typical results are shown in Fig. 2. The effect of geometric parameters on the magnitude of the gradient is apparent on inspection of the figure, in which the curves are labeled by two numbers in parentheses; the first gives the value of H and the second the value of R.

With the effective radiative density known for all surfaces inside the chamber, the steady-state density near any point $p(z, r, \phi)$ exposed to the source and/or reflecting walls can be calculated by the relationship[4]

$$n(z, r, \phi) = (1/4\pi) \int n_s \, d\omega_s, \tag{3}$$

where n_s represents the effective radiative density associated with an element of surface area S on the reflecting wall or source, $d\omega_s$ is the element

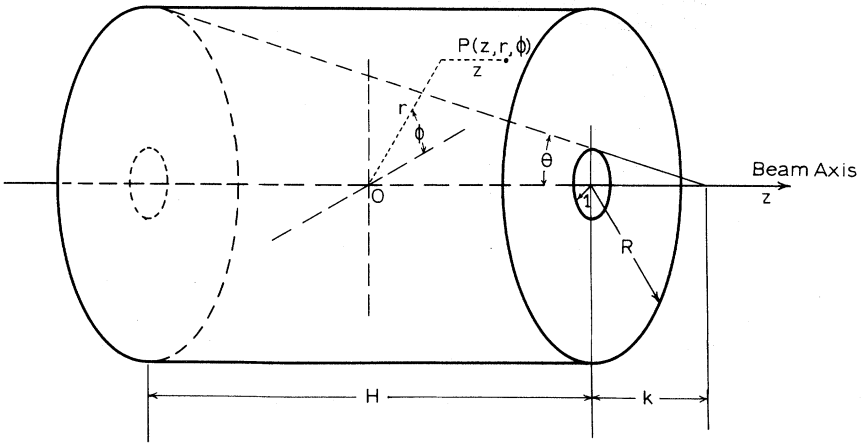

FIG. 1. Scattering chamber with thin circular apertures of unit radius. The gas source at uniform number density n_0 is bounded by the cylindrical wall $r=R$ inside the chamber.

of solid angle subtended at P by S, and the integral is to be evaluated over all of the source and walls directly exposed to P.

For the present geometry using Eq. (2), Eq. (3) can be directly integrated for points lying on the beam axis ($r=0$). The process is simplified by the variable change $p=z+\frac{1}{2}H$ in terms of which the integrated result is

$$n^*(p)=n(p)/n_0=(\tfrac{1}{2}p)[A(p)+B(p)], \qquad (4)$$

where

$$A(p)=\frac{a_0+a_1-p^2(a_2+a_3)}{(p^2+1)^{1/2}}$$

$$-[a_2+\tfrac{1}{2}a_3+(\tfrac{3}{2}a_3p^2-a_1)\sinh^{-1}(1/p)](p^2+1)^{1/2},$$

and the form of $B(p)$ depends on whether or not the axial point is directly exposed to radiations from the source [i.e., on the sign of $p-(H+k)$, Fig. 1]:

$$B(p\leq H+k)=\frac{1-a_0-a_1R+a_2p^2}{(p^2+R^2)^{1/2}}$$

$$+(a_2+\tfrac{1}{2}a_3R+a_3Rp^2)(p^2+R^2)^{1/2}$$

$$+(a_1-\tfrac{3}{2}a_3p^2)\sinh^{-1}(R/p)$$

$$-\frac{(p-H)}{[(p-H)^2+\delta^2]^{1/2}},$$

where

$\delta=R$ for $p<H$

$=1$ for $p>H$,

and

$$B(p>H+k)=\frac{a_2+a_3p^2}{[2(p-H)^2]}[(p-H)^2+1]^{1/2}$$

$$-\frac{a_0(p-H)/p+a_1-a_2p(p-H)-a_3p^2}{[(p-H)^2+1]^{1/2}}$$

$$+(a_1-3a_3\tfrac{1}{2}p^2)\sinh^{-1}\left(\frac{1}{(p-H)}\right).$$

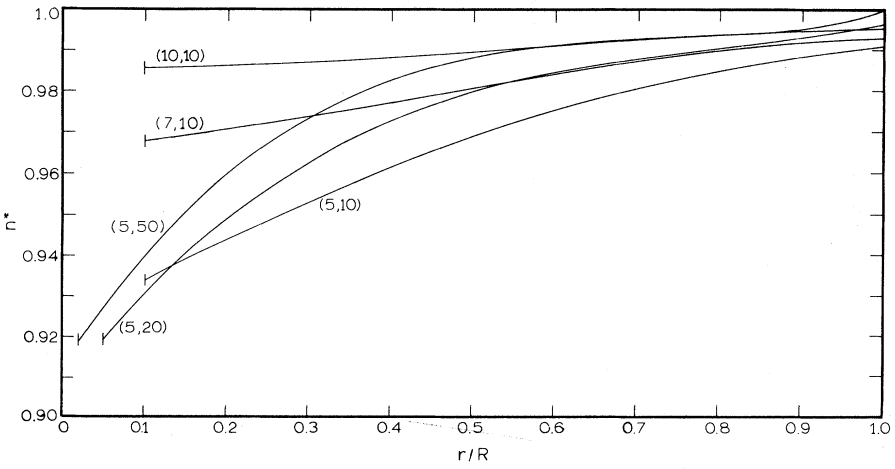

FIG. 2. Typical effective-radiative-density gradients on interior ends of scattering chambers identified by reduced geometry parameters (H, R).

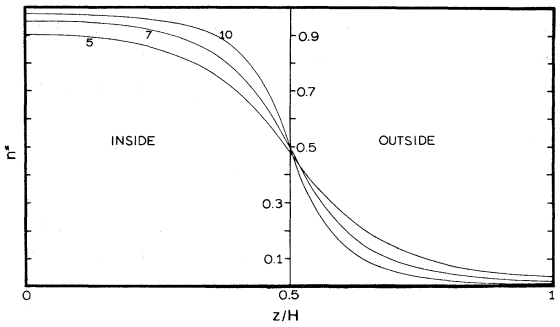

FIG. 3. Typical reduced-density profiles along the beam axis for scattering chambers having reduced radius $R=10$ and reduced lengths $H=5$, 7, and 10.

Some typical axial density profiles are shown in Fig. 3. For the present case the next step, the evaluation of $\int_{-\infty}^{\infty} n^*(z)\,dz$, can be performed analytically. The result is given in terms of cell geometry parameters, including the angle θ between the beam axis and the straight line marking the limit of visibility of the source from the beam axis, Fig. 1:

$$\int_{-\infty}^{\infty} n^*(z)\,dz = I_{\text{source}} + a_0 I_0 + a_1 I_1 + a_2 I_2 + a_3 I_3, \tag{5}$$

where

$$I_{\text{source}} = (R-1)(\csc\theta - 1),$$

$$I_0 = H - I_{\text{source}},$$

$$I_1 = H - \tfrac{1}{2}(R^2-1)(\csc\theta - 1) + \tfrac{1}{2}H^2 \sinh^{-1}(\tan\theta),$$

$$I_2 = (R^2-1)(\tfrac{2}{3}\csc^3\theta - \csc\theta + \tfrac{1}{3}) + H - \tfrac{2}{3}H^3 - 2HR\cot\theta\csc\theta + H^2 \sinh^{-1}(\tan\theta),$$

and

$$I_3 = (R^4-1)[\tfrac{1}{4} + \tfrac{3}{8}\csc^3\theta - \tfrac{5}{8}\csc\theta - \tfrac{3}{8}\cot^4\theta \sinh^{-1}(\tan\theta)] + (H + \cot^3\theta + \tfrac{3}{2}H\cot^2\theta + H^2\cot\theta)\tfrac{3}{2}H\sinh^{-1}(\tan\theta) + \tfrac{13}{16}H - \tfrac{3}{2}H\csc\theta(\cot\theta - \tfrac{3}{2}H) - H^3(2 - \tfrac{1}{2}\sec\theta).$$

The terms I_{source}, I_0, I_1, I_2, and I_3 give the contribution to the definite integral due to the source region and the four separate terms in Eq. (2), respectively.

IV. RESULTS

Following the pattern of Paper II we define the correction factor α such that

$$\int_{-\infty}^{\infty} n(z)\,dz = \alpha n_0 l,$$

where l is the length of the scattering chamber. In terms of the present notation

$$\alpha = \int_{-\infty}^{\infty} n^*(z)\,dz/H.$$

Values of α are given in Table I for several geometries with reduced dimensions R and H in the ranges 10–100 and 1–13, respectively. Values of α near unity are favored by small R and large H. Although this result suggests that such geometries should be used experimentally to avoid the need for a substantial density profile correction, it is worthy of note that reliable correction factors would permit the use of much shorter scattering chambers and correspondingly higher source pressures. This should prove to be the most significant utility of computed α values since uncertain pressure measurement is the weakest factor in computation of total scattering cross sections from experimental data, and the reliability of pressure measurements increases with increasing pressure.

TABLE I. Correction factor α as a function of reduced scattering chamber length H and radius R.

H \ R	10	20	30	40	50	60	70	80	90	100
1	0.6400	0.6073								
2	0.8371	0.8010	0.7917	0.7887	0.7879	0.7892				
3	0.9169	0.8908	0.8812	0.8771	0.8749	0.8731	0.8711	0.8688	0.8682	0.8663
4	0.9520	0.9351	0.9270	0.9230	0.9209	0.9195	0.9182	0.9164	0.9149	0.9122
5	0.9693	0.9586	0.9522	0.9581	0.9467	0.9454	0.9446	0.9436	0.9428	0.9410
6	0.9790	0.9719	0.9671	0.9641	0.9623	0.9611	0.9604	0.9597	0.9592	0.9583
7	0.9849	0.9800	0.9764	0.9739	0.9723	0.9712	0.9705	0.9700	0.9696	0.9691
8	0.9888	0.9852	0.9824	0.9804	0.9790	0.9780	0.9774	0.9769	0.9765	0.9761
9	0.9914	0.9887	0.9865	0.9849	0.9837	0.9828	0.9822	0.9817	0.9814	0.9811
10	0.9933	0.9911	0.9894	0.9881	0.9871	0.9863	0.9857	0.9853	0.9850	0.9847
11	0.9947	0.9929	0.9915	0.9904	0.9856	0.9889	0.9884	0.9880	0.9870	0.9874
12	0.9957	0.9942	0.9931	0.9922	0.9914	0.9909	0.9904	0.9900	0.9897	0.9895
13	0.9965	0.9952	0.9942	0.9935	0.9929	0.9924	0.9920	0.9916	0.9914	0.9911

It is for this reason that calculations are presently under way for other practical geometries, including scattering chambers with rectangular slits and chambers with apertures of finite channel length. Results of these calculations will be the subjects of future reports.

In a separate article[5] we are reporting the results of our absolute total scattering cross section measurements for the system $Cs \rightarrow CH_3CCl_3$ where α correction has been applied. It is suggested that we can also extract information about reactive scattering cross sections from such precise absolute total cross section measurements.

ACKNOWLEDGMENT

We are thankful to the University of Florida Computing Center for financial help in carrying out this work.

---

*Present address: Institute of Gas Technology, 3424 South State Street, Chicago, Ill. 60616.

[1]B. P. Mathur and S. O. Colgate, Phys. Rev. A 6, 1266 (1972), hereafter referred to as Paper I.

[2]R. N. Nelson and S. O. Colgate, Phys. Rev. A 8, 3045 (1973), hereafter referred to as Paper II.

[3]S. O. Colgate and T. C. Imeson, J. Chem. Phys. 53, 1270 (1970).

[4]S. O. Colgate, Vacuum 21, 483 (1972).

[5]B. P. Mathur, J. E. Field, and S. O. Colgate (unpublished).